

1990

Three-Dimensional Current Distributions in a Bipolar, Chlor-Alkali Membrane Cell

Ralph E. White

University of South Carolina - Columbia, white@cec.sc.edu

F. Jagush

Texas A & M University - College Station

H. S. Burney

Follow this and additional works at: https://scholarcommons.sc.edu/eche_facpub

 Part of the [Chemical Engineering Commons](#)

Publication Info

Journal of the Electrochemical Society, 1990, pages 1846-1848.

© The Electrochemical Society, Inc. 1990. All rights reserved. Except as provided under U.S. copyright law, this work may not be reproduced, resold, distributed, or modified without the express permission of The Electrochemical Society (ECS). The archival version of this work was published in the *Journal of the Electrochemical Society*.

<http://www.electrochem.org/>

DOI: 10.1149/1.2086814

<http://dx.doi.org/10.1149/1.2086814>

This Article is brought to you by the Chemical Engineering, Department of at Scholar Commons. It has been accepted for inclusion in Faculty Publications by an authorized administrator of Scholar Commons. For more information, please contact digres@mailbox.sc.edu.

$\bar{C}_{a_i}^*$	velocity-averaged concentration near the anode, mol/cm ³	ϕ_4	electrolyte potential at interface between diffusion region and perfectly mixed region on cathode side, V
$\bar{C}_{c_i}^*$	velocity-averaged concentration near the cathode, mol/cm ³	$\Delta\phi$	voltage drop through electrolyte and separator, V
E_{cell}	operating potential of reactor, V	ϵ_C	current efficiency (6)
i	total current density, A/cm ²	ϵ_T	total efficiency (6)
L	reactor length, cm		
n	number of components		
N_M	Macmullin number		
q_A	volumetric flow rate through anode side, cm ³ /s		
q_C	volumetric flow rate through cathode side, cm ³ /s		
S_A	distance from anode surface to separator, cm		
S_C	distance from cathode surface to separator, cm		
S_S	distance across separator, cm		
t	time, s		
T	reactor temperature, K		
U_a	potential at anode, V		
U_c	potential at cathode, V		
V_{TA}	volume of storage tank on anode side, cm ³		
V_{TC}	volume of storage tank on cathode side, cm ³		
\bar{v}_a	average velocity through anode side, cm/s		
\bar{v}_c	average velocity through cathode side, cm/s		
β	area ratio for porous electrode, A_{eff}/A		
δ_A	diffusion layer thickness near anode, cm		
δ_C	diffusion layer thickness near cathode, cm		
μ	ratio of residence times, cathodic side/anodic side (see Eq. [4])		
τ	dimensionless time (see Eq. [3])		
ϕ_a	electrolyte potential at anode surface, V		
ϕ_c	electrolyte potential at cathode surface, V		
ϕ_1	electrolyte potential at interface between diffusion region and perfectly mixed region on anode side, V		
ϕ_2	electrolyte potential at separator on anode side, V		
ϕ_3	electrolyte potential at separator on cathode side, V		

REFERENCES

1. J. Lee and J. R. Selman, *This Journal*, **129**, 1670 (1982).
2. J. Lee and J. R. Selman, *ibid.*, **130**, 1237 (1983).
3. J. Lee, Ph. D. Dissertation, Illinois Institute of Technology, Chicago, IL (1981).
4. J. W. Van Zee, R. E. White, P. Grimes, and R. Bellows, in "Electrochemical Cell Design," R. E. White, Editor, p. 293, Plenum Publishing Co., New York (1984).
5. M. J. Mader and R. E. White, *This Journal*, **133**, 1297 (1986).
6. T. I. Evans and R. E. White, *ibid.*, **134**, 866 (1987).
7. T. I. Evans and R. E. White, *ibid.*, **134**, 2725 (1987).
8. M. Eigen and K. Kustin, *J. Am. Chem. Soc.*, **84**, 1355 (1962).
9. D. J. Pickett, "Electrochemical Reactor Design," Chap. 4-6, Elsevier Scientific Publishing Co., New York (1979).
10. J. S. Newman, "Electrochemical Systems," Chap. 11, Prentice-Hall Inc., Englewood Cliffs, NJ (1973).
11. V. Edwards and J. S. Newman, *This Journal*, **134**, 1181 (1987).
12. T. V. Nguyen, C. W. Walton, and R. E. White, *ibid.*, **133**, 1130 (1986).
13. G. D. Simpson and R. E. White, *ibid.*, **136**, 2137 (1989).
14. G. D. Simpson, M. S. Thesis, Texas A & M University, College Station, TX (1988).

Technical Notes



Three-Dimensional Current Distributions in a Bipolar, Chlor-Alkali Membrane Cell

R. E. White* and F. Jagush**

Department of Chemical Engineering, Texas A&M University, College Station, Texas 77843-3122

H. S. Burney*

Dow Chemical U.S.A., Texas Applied Science Laboratories, Freeport, Texas 77541

The current distributions in a stack of bipolar, membrane chlor-alkali cells are important design considerations (1). The degree of nonuniformity of the current distribution is important to know because highly nonuniform current distributions could cause, among other things, severe damage to the membrane in a cell stack (2).

Recently, Dimpault-Darcy and White (3) used a computer program named TOPAZ2D (4), which is based on the finite element technique, to predict the two-dimensional current and potential distributions in a bipolar plate electrolyzer. In that paper they stated that TOPAZ3D (5) could be used to predict current and potential distributions for three spatial coordinates, but they did not present any results.

The finite element method has also been used by others (6-12) to predict current and potential distributions. However, most of these investigators used two spatial coordinates in their work. They used a two-dimensional method

to predict current and potential distributions in chlorine cells (6, 7), electroplating cells (8-10), and corrosion processes (11, 12). Morris and Smyrl (12) did use three spatial coordinates in some of their work, but they did not consider the spatial dependence of the specific conductivities, as done here. The purpose of this paper is to present the current distributions obtained by using TOPAZ3D for a three-dimensional section of bipolar, membrane chlor-alkali cell which includes portions that have spatial-dependent specific conductivities.

Figure 1 is a schematic of the section of a bipolar membrane cell (see Ref. (1) and (13) for a description of the cell) considered here. As shown in Fig. 1, a set current enters the anode from the boss portion of an anode/cathode element of the stack, passes through the various regions of the cell, and leaves through the boss portion of the next anode/cathode element. Only one quarter of a boss and the associated cell components are considered because of the symmetry of the components in the middle of the cell. Even though the results presented below do not apply to sections of the cell near the edge of the stack, the tech-

* Electrochemical Society Active Member.

** Electrochemical Society Student Member.

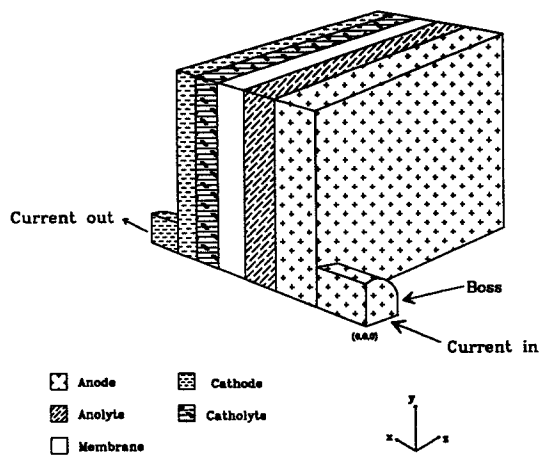


Fig. 1. Schematic of a cell section (not to scale)

nique could be used to study those sections, if desired. The number and placement of the bosses (or gophers as they are sometimes called) affects significantly the current distribution in the cells; however, this is not considered in this paper.

It is not shown in Fig. 1, but the anodes and cathodes used in these cells are made of expanded metal. Consequently, the effective conductivity of each electrode depends on direction. This complexity was included in the model of the cell.

Method

Steady-state three-dimensional current and potential distributions in electrolysis cells can be predicted by using the heat transfer code called TOPAZ3D (5). The procedure for this consists of casting the charge transfer problem into a form suitable for solution by using the heat transfer program. This can be done by recognizing that charge is conserved in the region of interest and writing the appropriate equations to describe this. Charge will be conserved in a region Ω if the divergence of the current density in that region is zero

$$\nabla \cdot i = 0 \text{ in } \Omega \quad [1]$$

where i is given by Ohm's law.

$$i = i_x + i_y + i_z = - \left(\kappa_x \frac{\partial \Phi}{\partial x} + \kappa_y \frac{\partial \Phi}{\partial y} + \kappa_z \frac{\partial \Phi}{\partial z} \right) \quad [2]$$

Substitution of Eq. [2] into Eq. [1] yields the governing equation for the potential Φ at steady-state conditions

$$\frac{\partial}{\partial x} \left(\kappa_x \frac{\partial \Phi}{\partial x} \right) + \frac{\partial}{\partial y} \left(\kappa_y \frac{\partial \Phi}{\partial y} \right) + \frac{\partial}{\partial z} \left(\kappa_z \frac{\partial \Phi}{\partial z} \right) = 0 \text{ in } \Omega \quad [3]$$

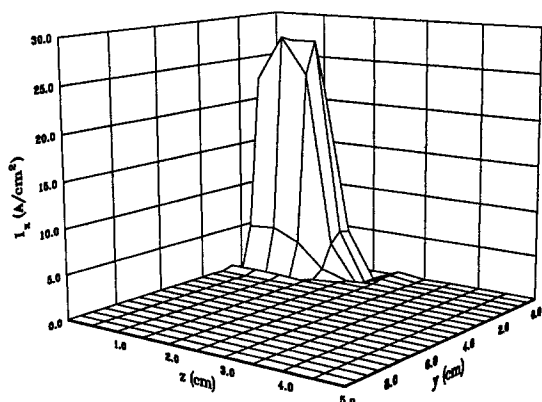


Fig. 2. Current distribution in the x direction on the back side of the anode.

On a surface segment Γ_i of the solid Ω , it is assumed here that charge transfer can be represented by

$$\kappa_x \frac{\partial \Phi}{\partial x} n_x + \kappa_y \frac{\partial \Phi}{\partial y} n_y + \kappa_z \frac{\partial \Phi}{\partial z} n_z = i_{s,i} \text{ on } \Gamma_i \quad [4]$$

where $i_{s,i}$ is the current density in A/cm^2 and is determined by dividing the set current that passes through Γ_i by the projected area of that surface segment. Insulated surfaces (or surfaces of symmetry) are handled by setting $i_{s,i}$ equal to zero.

TOPAZ3D can be used to determine $\Phi(x, y, z)$ and then i by using the dimensionless temperature option. This selection means that the dependent variable in TOPAZ3D must be dimensionless. Consequently, it is necessary to make Φ dimensionless. One way to do this is to define a reference potential Φ_{ref} and use it to make Φ dimensionless

$$\phi = \Phi/\Phi_{ref} \quad [5]$$

Substitution of Eq. [5] into Eq. [3] and [4] yields

$$\frac{\partial}{\partial x} \left(\kappa_x \frac{\partial \phi}{\partial x} \right) + \frac{\partial}{\partial y} \left(\kappa_y \frac{\partial \phi}{\partial y} \right) + \frac{\partial}{\partial z} \left(\kappa_z \frac{\partial \phi}{\partial z} \right) = 0 \text{ in } \Omega \quad [6]$$

and

$$\kappa_x \frac{\partial \phi}{\partial x} n_x + \kappa_y \frac{\partial \phi}{\partial y} n_y + \kappa_z \frac{\partial \phi}{\partial z} n_z = i_{s,i}/\Phi_{ref} \text{ on } \Gamma_i \quad [4]$$

Results and Discussion

Values for ϕ can be found by using TOPAZ3D after specifying the geometry and surfaces of the region Ω and selecting values for $\kappa_x, \kappa_y, \kappa_z, i_{s,i}$ and Φ_{ref} . If the region Ω consists of several different parts, the values for the specific conductivities for each region must be specified. This can be done easily by utilizing INGRID (14) to prepare the finite element grid for all of the parts of the cell section shown in Fig. 1.

Figures 2 and 3 show the current distributions of the back side and front side of the anode, respectively, which were obtained by using input values appropriate for the cell segment shown in Fig. 1. For example, the anode considered here was of the expanded metal DSA® type. To account for this in the model, values for the specific conductivities in the $x, y,$ and z directions were set as follows: $\kappa_x = 1.03 \times 10^4 \Omega^{-1} \text{ cm}^{-1}$, $\kappa_y = 1.26 \times 10^4 \Omega^{-1} \text{ cm}^{-1}$, and $\kappa_z = 1.98 \times 10^3 \Omega^{-1} \text{ cm}^{-1}$. The other input values used for the case presented here are available from the authors upon request. As can be seen by comparison of Fig. 2 and 3, the nonuniform current density distribution on the back side of the anode becomes relatively uniform on the front side. This is due to the highly conductive material used as the anode. Similar plots (not presented here) show that the current density distribution through the membrane is essentially uniform for this cell configuration and current

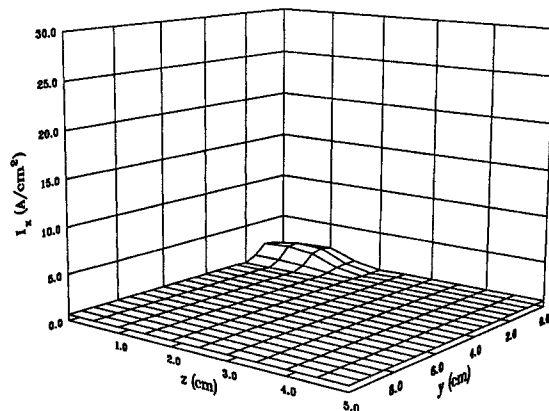


Fig. 3. Current distribution in the x direction on the front side of the anode.

density; and, consequently, should prevent overheating or blistering of the membrane and damage to the membrane due to nonuniform current distributions and impurities.

Summary

TOPAZ3D (5) can be used to determine current density distributions in electrolysis cells as demonstrated for a section of a bipolar, chlor-alkali membrane cell. The current density for the electrolysis cell considered here was about 0.62 A/cm². The resulting current density in a typical boss portion of the cell was about 25 A/cm². However, because of the highly conductive electrodes used in the cell, the current density distribution through the membrane portion of the cell was found to be essentially uniform.

Acknowledgment

The authors acknowledge gratefully that this work was supported by the Texas Applied Science and Technology Laboratories of Dow Chemical U.S.A.

Manuscript submitted June 26, 1989; revised manuscript received Dec. 8, 1989.

Dow Chemical U.S.A. assisted in meeting the publication costs of this article.

LIST OF SYMBOLS

\mathbf{i}	current density vector, A/cm ²
$i_{s,i}$	current density on surface segment i , A/cm ²
n_x, n_y, n_z	dimensionless directional cosines
$x, y, \text{ and } z$	coordinates in cm
Greek	
$\kappa_x, \kappa_y, \kappa_z$	specific conductivities, $\Omega^{-1} \text{ cm}^{-1}$
Φ	potential, V
Φ_{ref}	reference potential ($\Phi_{\text{ref}} = 1\text{V}$ here), V
ϕ	dimensionless potential
Ω	region of interest
Γ_i	surface segment i on Ω

REFERENCES

1. G. J. Morris, in "Modern Chlor Alkali Technology," Vol. 4, K. Wall, Editor, Ellis Horwood Limited, West Sussex, England (1989).
2. J. T. Keating, in "Electrochemical Engineering in the Chlor-Alkali and Chlorate Industries," PV 88-2, F. Hine, W. B. Darlington, R. E. White, and R. D. Varjian, Editors, p. 311, The Electrochemical Society Softbound Proceedings Series, Pennington, NJ (1988).
3. E. C. Dimpault-Darcy and R. E. White, *This Journal*, **135**, 656 (1988).
4. A. B. Shapiro, "TOPAZ2D—A Two-Dimensional Finite Element Code for Heat Transfer Analysis, Electrostatic, and Magnetostatic Problems," University of California, Lawrence Livermore National Laboratory, Report No. UCID-20824 (1986).
5. A. B. Shapiro, "TOPAZ3D—A Three-Dimensional Finite Element Heat Transfer Code," University of California, Lawrence Livermore National Laboratory, Report No. UCID-20484 (1985).
6. J. Deconinck, D. Maggetto, and J. Verechken, *This Journal*, **132**, 2960 (1985).
7. M. Simek, and I. Rousar, *J. Applied Electrochem.*, **18**, 96 (1988).
8. R. Alkire and T. Bergh, *This Journal*, **125**, 1981 (1978).
9. M. Matlosz, C. Creton, C. Clerc, and D. Landolt, *ibid.*, **134**, 3015 (1987).
10. N. G. Zamani, J. M. Chuang, and C. C. Hsiung, *Int. J. Num. Methods Eng.*, **24**, 1479 (1987).
11. N. G. Zamani, J. F. Porter, and A. A. Mufti, *ibid.*, **23**, 1295 (1986).
12. R. Morris and W. Smyrl, *AIChE J.*, **34**, 723 (1988).
13. G. J. E. Morris, J. R. Pimlott, R. N. Beaver, H. D. Dang, and S. Grosshandler, U.S. Pat. 4,604,171 (1986).
14. D. W. Stillman and J. O. Hallquist, "INGRID: A Three-Dimensional Mesh Generator for Modeling Non-linear Systems," University of California, Lawrence Livermore National Laboratory, Report No. UCID-20506 (1985).

Predicted Secondary Current Distributions for Linear Kinetics in a Modified Three-Dimensional Hull Cell

F. A. Jagush* and R. E. White**

Department of Chemical Engineering, Texas A&M University, College Station, Texas 77843-3122

William E. Ryan**

Texas Instruments, Incorporated, Dallas, Texas 75265

Current density distribution is an important consideration for those involved in designing electrochemical systems and electroplating systems in particular. Although it is important, the common practice in industry is to use trial and error to determine designs that optimize current density distributions in electroplating. The purpose of this paper is to illustrate the use of the finite element method (FEM) to predict three-dimensional current density distributions.

Two-dimensional FEM has been used successfully in modeling corrosion systems (1-8), electrolyzers (9), and three-phase cells (10, 11). Alkire, Bergh, and Sani (12) were among the first to apply the finite element method to electrochemical potential distribution problems. They studied the shape changes in electrodes during electrodeposition. The system studied was composed of a cathode made with parallel metal strips separated by an insulator and an anode at a fixed distance. Transient analysis using the FEM provided a time history of cathode shape during deposition. Finite element results agreed to within 2-5% of the analytical solutions. Micromechanics of multilayer printed

wiring boards have also been studied using the FEM. Lee *et al.* (13) studied the thermomechanical strain in printed wiring boards. They constructed a finite element model for both plated through-holes and buried via structures to calculate the stresses in the copper barrel and at the via junctions.

An illustrative example of the use of the FEM in electroplating is given by Matlosz *et al.* (14). In their paper they compared the finite element solution of current densities in a Hull cell to those obtained experimentally and through the boundary element method (BEM). The Hull cell is used commonly for visual measurement of the quality of electrochemical solutions (15). Most plating solutions are tested using a current of 2A and a plating time of 10 min (16). The slanted cathode used in this cell allows for a range of current densities, and how much of it is covered with deposit will depend on the quality of the solution.

TOPAZ2D (17) and TOPAZ3D (18) are finite element codes designed specifically for heat transfer problems. White *et al.* (19) used TOPAZ3D to predict current and potential distributions in a bipolar chlor-alkali membrane cell. They also present an example of the use of INGRID (20), a program that serves as preprocessor to TOPAZ3D. Topaz programs have a feature that most other finite ele-

* Electrochemical Society Student Member.

** Electrochemical Society Active Member.